

Scattering on the lateral one-dimensional superlattice with spin-orbit coupling

D.V. Khomitsky*

*Department of Physics, University of Nizhny Novgorod,
23 Gagarin Avenue, 603950 Nizhny Novgorod, Russian Federation*

(Dated: May 25, 2019)

The problem of scattering for two-dimensional electron gas with Rashba spin-orbit coupling on the lateral one-dimensional superlattice with spin-orbit Rashba Hamiltonian is considered. The transmitted states in the superlattice are the Bloch spinors with the spin split band structure. The orientation angles of incoming states giving the propagation and total reflection are found for different momenta and polarization of incident electrons. For the propagating states in the superlattice the mean spin values are calculated as a function of the incoming state momenta and possible spin filtration mechanism is discussed.

PACS numbers: 72.25.Dc, 72.25.Mk, 73.21.Cd

I. INTRODUCTION

In two-dimensional semiconductor heterostructures the spin-orbit interaction (SO) is usually dominated by the Rashba coupling¹ coming from the structure inversion asymmetry of confining potential and effective mass difference. The interest to these structures is usually related to the possible effects in charge and spin transport which produce novel ideas on how to control the spins in semiconductor structures and give rise to the applications of spintronics.² One of the first possible applications was the principle of the spin field-effect transistor proposed by Datta and Das³ who investigated the ballistic transport of spin-polarized electrons through quasi one-dimensional (1D) channel composed of a series of segments with and without spin-orbit interaction. They considered the lateral interface between two regions with different strengths of the spin-orbit interaction which can be used to control the electron spin in gated two-dimensional semiconductor heterostructures. For a beam with a nonzero angle of incidence, the transmitted electrons will split into two spin polarization components propagating at different angles. Later, the low-dimensional semiconductor structures with SO interaction were studied theoretically in numerous papers^{4,5,6,7,8,9,10} including the 1D periodic systems with SO coupling.^{8,10} In particular, the transmission coefficient of quasi 1D periodic system consisting of segments with different SO coupling constant has been calculated.⁸ It should be mentioned that the strength of Rashba SO coupling in a gated structure can be modified by the external gate potential for up to 50%¹¹ which makes reasonable the investigation of gated structures with varying SO strength. The idea to control the spin orientation in the beam of particles by means of SO coupling has been proposed also in terms of spin optics.^{12,13} In particular, the scattering on the border of two half-spaces each having a different value of SO coupling constants was studied.¹² It was shown that the spin orientation in transmitted wave strongly depends on the chirality of the incident one as well as on the angle of incidence and the angles of total reflection exist. Later the same authors applied their results for the case of spin

polarizing in a system consisted of ballistic and diffusive regions.¹³ Nowadays the problem of new structures and schemes to be proposed for the application of SO interaction for control of the spin degrees of freedom without applying the external magnetic field remains to be actual. One of the possible ways can be found in application of gated structures with externally tuned periodic electric potential.

In our recent paper we studied quantum states and the electron spin distribution in a system combining the spin-splitting phenomena caused by the SO interaction and the external gate-controlled periodic electric potential.¹⁴ We investigated the Bloch spinors and spin polarization that can be achieved in currently manufactured gated semiconductor structures with lateral superlattice. Such 1D superlattice can be fabricated by the metal gate evaporation with typical period of 50 – 200 nm. We used the value of lateral period in the x -direction to be $a = 60$ nm which gives us the energy scale $\pi^2 \hbar^2 / 2ma^2$ of the order of 2 meV for the effective mass $m = 0.067m_0$ in GaAs. Such energy scale means that the wavevector is measured in units of π/a , leading to typical energies of 2D electron gas (2DEG) to be of the order of 10 meV. The values of Rashba coupling constant for the most important semiconductors is in the range of $1 - 5 \cdot 10^{-11}$ eVm. We use the biggest value $\alpha = 5 \cdot 10^{-11}$ eVm in our calculations to be the SO effects more pronounced which gives the typical shift of the energy dispersion curves k_{SO} to be of the order of π/a . Thus, the electron kinetic energy $\pi^2 \hbar^2 k^2 / 2m$ in the structure will be comparable to the Rashba energy αk which will help to distinguish the effects of SO interaction and periodic potential. It should be mentioned also that the energy scale of 10 meV means that the effects in SO superlattices discussed here can be clearly observed experimentally at helium temperatures.

In the present paper we make an extensive use of our results for the quantum states in SO superlattice¹⁴ for investigation of the problem of scattering on the SO superlattice of the beam of electrons which is initially polarized by the Rashba SO interaction. We solve the scattering problem on the SO superlattice occupying a half-space and study the transmitted states as a function of the

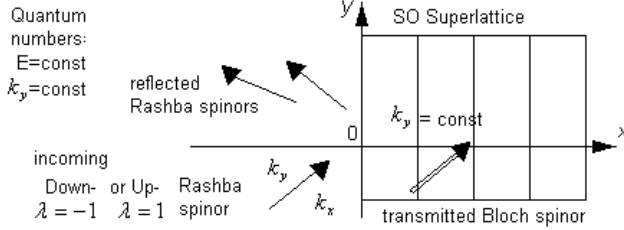


FIG. 1: Geometry of scattering of two-component spinors on the spin-orbit lateral superlattice. The incoming and reflected spinors are the eigenstates of Rashba Hamiltonian while the transmitted ones are the Bloch spinors. For each polarization of incoming state there are two reflected states corresponding to two bands of Rashba Hamiltonian.

wavevectors and Fermi energy of the incoming states. We see how the gaps in the energy band spectrum of the SO superlattice manifest themselves in the existence of total reflection areas for some of the incident wavevectors and how the polarization of the incoming states is imprinted in the spin polarization of transmitted states. The distribution of spins in transmitted states for the different polarization of incoming ones suggests some further ideas for controllable spin filtration by means of SO superlattice.

The paper is organized as follows. In Sec.II we outline the geometry of our structure and introduce the scattering scheme on the SO superlattice. In Sec.III we show how the quantum states in the SO superlattice look like and present an example of energy spectrum. In Sec.IV we solve the problem of scattering on the border of the free 2D electron gas with Rashba SO interaction and the half-infinite SO superlattice. The results are used in Sec.V for calculation of the mean spin values for the transmitted state. We also investigate the possible applications of our system for the practical spin filtration. Finally, the conclusions are given in Sec.VI.

II. STRUCTURE GEOMETRY AND SCATTERING SCHEME

We consider the scattering of electrons with spin-orbit coupling described by the two-component spinors on the one-dimensional superlattice occupying a half-space and also having a spin-orbit Rashba term in the Hamiltonian. The incoming and reflected spinors are the eigenstates of Rashba Hamiltonian while the transmitted ones are the Bloch spinors with each of the components possessing the Bloch theorem. The scheme of structure geometry for our problem is presented in Fig.1.

The half-space $x < 0$ is the semiconductor structure with 2DEG characterized by the effective mass m and Rashba spin orbit coupling strength α . The quantum states here are the eigenstates of the Hamiltonian ($\hbar = 1$)

$$\hat{H}_0 = \frac{\hat{p}^2}{2m} + \alpha(\hat{\sigma}_x \hat{p}_y - \hat{\sigma}_y \hat{p}_x). \quad (1)$$

The eigenstate of (1) labeled by the momentum $\mathbf{k}_0 = (k_x, k_y)$ and the polarization index $\lambda = \pm 1$ has the following form:

$$x < 0 : \quad \psi_{\text{in}} = \frac{e^{i\mathbf{k}_0 \mathbf{r}}}{\sqrt{2}} \begin{pmatrix} 1 \\ \lambda e^{i\theta_0} \end{pmatrix} \quad (2)$$

where $\theta_0 = \arg[k_y - ik_x]$, and the energy of the state is

$$E_0(\mathbf{k}, \lambda) = \frac{k^2}{2m} + \lambda \alpha k. \quad (3)$$

The value $\lambda = -1$ labels the state with negative y projection of the spin for positive k_x and $k_y = 0$ and thus it is usually described as Rashba "down" polarized state while the value $\lambda = 1$ labels the Rashba "up" polarized state. The angle of incidence for the incoming wave is defined as $\arctan(k_y/k_x)$ for both polarizations. The incoming state is scattered on the border of the SO superlattice occupying the area at $x > 0$. In the left part of the space $x < 0$ there is the reflected state which is the linear combination of all eigenstates of (1) with the same energy as the incoming state and with $k_x < 0$ since the reflected states are moving to the left. Since the Rashba Hamiltonian (1) is two-fold degenerate both for $k_x > 0$ or $k_x < 0$, the reflected state consists of two spinors with the same energy as the incoming state but with different k_x -momenta belonging to different branches of Rashba Hamiltonian (1) with $\lambda = \mp 1^{12}$. The amplitudes $k_{1,2}$ of the k_x component of the momentum can be found at fixed k_y and E from (1) and are equal to

$$k_{1,2} = \sqrt{2mE + (\lambda\alpha)^2} \pm \lambda\alpha \quad (4)$$

where + and - refer to the down- and up- Rashba bands with $\lambda = \mp 1$. Thus, the reflected state at $x < 0$ has the following form:

$$x < 0 : \quad \psi_{\text{ref}} = r_1 \frac{e^{-ik_1 x + ik_y y}}{\sqrt{2}} \begin{pmatrix} 1 \\ -e^{i\theta_1} \end{pmatrix} + r_2 \frac{e^{-ik_2 x + ik_y y}}{\sqrt{2}} \begin{pmatrix} 1 \\ e^{i\theta_2} \end{pmatrix}. \quad (5)$$

Here the phases are defined by the momentum components as $\theta_{1,2} = \arg[k_y - ik_{1,2}]$ and $r_{1,2}$ are the reflection coefficients which will be found below.

On the right-hand side in Fig.1 at $x > 0$ the transmitted electrons travel through the SO superlattice. The transmitted state is the linear combination of the eigenstates of the SO superlattice with the energy equal to the energy of the incoming state:

$$x > 0 : \psi_{\text{transm}} = \sum_{j=1}^N c_j \psi(k_j, k_y) \quad (6)$$

where the coefficients c_j will be determined below and $\psi(k_j, k_y)$ are the eigenstates of the SO superlattice. They have different quasimomenta components $k_x = k_j$ for which the energy is equal to the energy of the incident wave, and the same k_y momentum component as in the incident wave since the structure is homogeneous along the y direction. To proceed, we need to discuss the structure of the eigenstates and the energy spectrum in the SO superlattice.

III. QUANTUM STATES OF THE SPIN-ORBIT SUPERLATTICE

Here we shall briefly describe the structure of quantum states of the 2DEG with Rashba SO interaction subject to the 1D electrostatic periodic potential generated by the lateral superlattice.¹⁴

The Hamiltonian of the problem is the sum of the Rashba Hamiltonian (1) and the one-dimensional periodic potential $V(x)$ of a 1D superlattice with the period a . The simplest approximation for the form of the periodic potential can be chosen as

$$V(x) = V_0 \cos \frac{2\pi x}{a}. \quad (7)$$

We construct the wavefunction as a superposition of two-component spinors (2) which are the eigenstates of the Rashba Hamiltonian (1). In the presence of the periodic potential the wavevectors of the basis states are shifted by the reciprocal lattice vector \mathbf{b} of the superlattice:

$$\mathbf{k}_n = \mathbf{k} + n\mathbf{b} = \left(k_x + \frac{2\pi}{a}n, k_y \right), \quad (8)$$

$n = 0, \pm 1, \pm 2, \dots$ The eigenstate thus has the form

$$\psi_{s\mathbf{k}} = \sum_{\lambda n} a_{\lambda n}^s(\mathbf{k}) \frac{e^{i\mathbf{k}_n \mathbf{r}}}{\sqrt{2}} \begin{pmatrix} 1 \\ \lambda e^{i\theta_n} \end{pmatrix}, \quad \lambda = \pm 1 \quad (9)$$

where \mathbf{k} is the quasimomentum in the 1D Brillouin zone, s is the band number, and $\theta_n = \arg[k_y - ik_{nx}]$. After substituting the wavefunction (9) into the Schrödinger equation the coefficients $a_{\lambda n}$ are determined by the standard eigenvalue problem

$$\sum_{\lambda' n'} [(E_{\lambda' n'}^R - E) \delta_{\lambda n \lambda' n'} + V_{\lambda n \lambda' n'}] a_{\lambda' n'}^s = 0, \quad (10)$$

where $E_{\lambda n}^R$ is the energy of a free Rashba quantum state (3) taken at the point in \mathbf{k} -space defined by (8), i.e.

$E_{\lambda n}^R = E_0(k_x + 2\pi n/a)$. The matrix elements in the system (10) have the form:

$$V_{\lambda n \lambda' n'} = V_0 A_{nn'} (1 + \lambda \lambda' e^{i(\theta_n - \theta_{n'})}), \quad (11)$$

$$A_{nn'} = \frac{1}{2} \delta_{n, n' \pm 1}, \quad n = n' \pm 1.$$

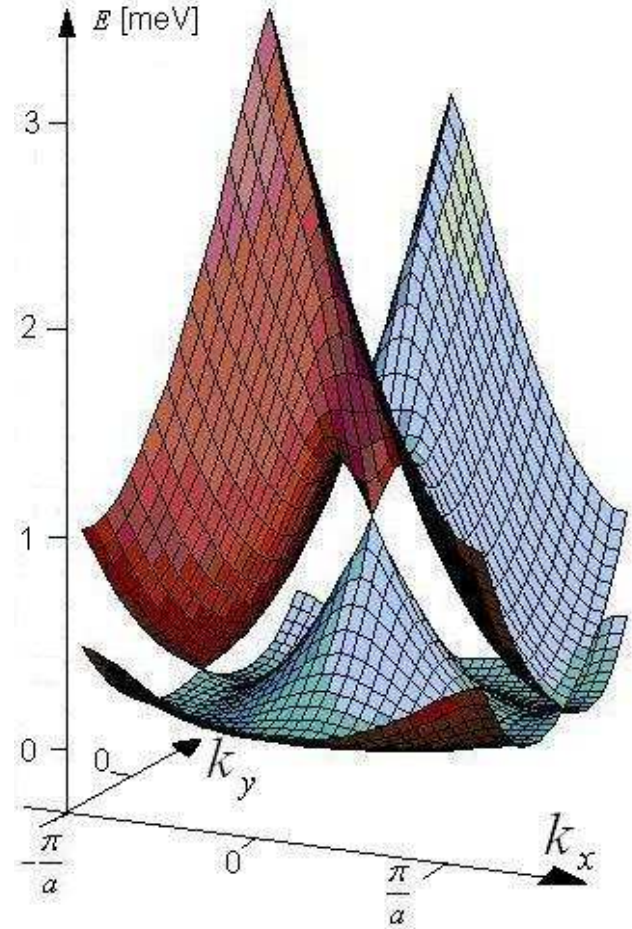


FIG. 2: Two lowest energy bands in a one-dimensional gated superlattice with spin-orbit coupling. The lattice period is $a = 60$ nm, the Rashba coupling constant $\alpha = 5 \cdot 10^{-11}$ eVm, and the amplitude of the periodic potential $V_0 = 2$ meV. The spectrum is shown as a function of quasimomentum k_x in the Brillouin zone and momentum k_y along the part of k_y axis.

In Fig.2 we give an example of energy spectrum $E(k_x, k_y)$. The parameters are the following: the superlattice period $a = 60$ nm, the Rashba coupling constant $\alpha = 5 \cdot 10^{-11}$ eVm, and the amplitude of the periodic potential $V_0 = 2$ meV. One can see that the spin degeneracy at $k_y = 0$ is not lifted at the center and at the borders of the BZ $k_x = \pm\pi/a$. The nature of this effect is due to the specific k_x and k_y dependence of matrix elements (11). The degeneracy at $k_y = 0$ is lifted at finite k_y by mutual influence of linear k_y terms in (1) and by the matrix elements (11). At certain conditions the anticrossing of the dispersion curves from different bands⁶

may take place. It should be mentioned that the value of SO constant α is chosen here to be close to the upper limit known for most popular semiconductors in order to make the visualization of SO effects more clear.

IV. CONTINUITY EQUATIONS FOR THE SCATTERING PROBLEM

The continuity equations at the scattering interface $x = 0$ follow from the Schrödinger equation and have the following form:¹²

$$\psi|_{x<0}^{x>0} = 0, \quad (12)$$

$$\left(\frac{\hat{p}_x}{m} - \alpha\hat{\sigma}_y\right)\psi|_{x<0}^{x>0} = 0. \quad (13)$$

They link the wavefunction $\psi_{\text{in}} + \psi_{\text{ref}}$ at the left half-space $x < 0$ and the wavefunction ψ_{transm} at the right half-space $x > 0$. Here the first equation for two-component spinors describes the continuity of the wavefunction while the second one corresponds to the continuity of the velocity. Since both of the equations in (13) are written for two-component spinors, one has totally four algebraic equations describing the scattering which can be easily solved.

The quantum numbers which remain to be good during the scattering on 1D superlattice parallel to x axis are the k_y component of the momentum and the energy of the incoming state. Here one has to distinguish the case when the energy of the incoming state at fixed k_y is within the limits of one of the superlattice bands and when this energy corresponds to a gap in the superlattice spectrum. The first case corresponds to the defined solution to system (13). For the second case the solution to the Schrödinger equation is not finite on the whole x axis and thus there are no states which propagate from the scattering interface through the superlattice. We call such case as a case of total reflection in analogy with optical scattering. It should be mentioned that such effect was already observed for the scattering of the Rashba states on the interface between two areas with different SO constant α .¹² The states which do not propagate through the superlattice and are localized at the interface border are known as Tamm states. Such states were studied previously both in bulk crystals^{15,16} and later in the superlattices.^{17,18,19} In the latter case it was shown that typically the Tamm states decay inside the superlattice on the length of several periods with different results varying from two - three¹⁷ to five - seven¹⁹ lattice periods. In our case these results mean that the typical penetration length of Tamm states will be of the order of 100 - 700 nm which is substantially smaller than the total length of superlattices actually used in the present experiments. Hence, there will be no detection of such states with the possible device mounted after the superlattice. Thus, we neglect the Tamm states localized at

the interface and consider only the Bloch states with the energy belonging to the bands of the superlattice which were discussed above.

V. SPIN POLARIZATION IN TRANSMITTED STATE

When the transmitted state (6) is fully determined, one can calculate the distribution of the mean spin values

$$\sigma_i(\mathbf{k}) = \langle \psi_{\text{transm}} | \hat{\sigma}_i | \psi_{\text{transm}} \rangle \quad (14)$$

for the transmitted state as a function of the wavevectors $\mathbf{k} = (k_x, k_y)$ of the incident state.

The spin distribution in the (k_x, k_y) plane labeling the incident wave for the Rashba states (2) is well-known and may be described as It is interesting to find now the distribution of spins in the transmitted state as a function of the point in the same plane (k_x, k_y) and polarization $\lambda = \mp 1$ describing the incident states. The distribution of spin mean values for the transmitted state as a function of the point in the (k_x, k_y) plane labeling the incident state is shown as vectors with (σ_x, σ_y) components in Fig.3. As in Fig.2, the amplitude of the periodic potential $V_0 = 2$ meV. Here Fig.3a corresponds to the initial "down" Rashba state with $\lambda = -1$ and Fig.3b is for the "up" Rashba state with $\lambda = 1$. The spins are shown in the interval of $k_{x,y}$ from 0 to $4\pi/a$. The reason for showing positive k_x only is that the incident state is coming from the left and thus $k_x > 0$. Then, the structure and the scattering is symmetrical with respect to y and k_y , respectively. Correspondingly, the whole interval of incident angles defined as $\arctan(k_y/k_x)$ is covered by positive k_x . The spin distribution for negative k_x can be obtained from Fig.3 by replacing σ_x spin projection to $-\sigma_x$. One can see in Fig.3 that the spin distribution is qualitatively modified by the superlattice which is tunable by the gate voltage. As a result, the controllable spin transmission can be achieved by SO superlattice linked to the semiconductor structure with SO coupling. The detailed spin distribution in the insets of Fig.3 is shown below in Fig.4a and Fig.5a, respectively.

By comparing Fig3a,b. one can see that the global spin vortex direction follows the one of the incoming state but the presence of the lateral superlattice is clearly observable. First of all, some of the initial states may have the energy which falls in the energy gap of the superlattice spectrum and thus no solution for the propagating wave inside the superlattice can be found. Such points are labeled by black circles and may be called the filtering points or points of the total reflection when no electrons with given polarizations are transmitted through the superlattice.

The relation of total reflection to the energy gaps of the superlattice is shown in Fig.4 and Fig.5. In Fig.4a and Fig.5a the detailed spin distributions are shown for the

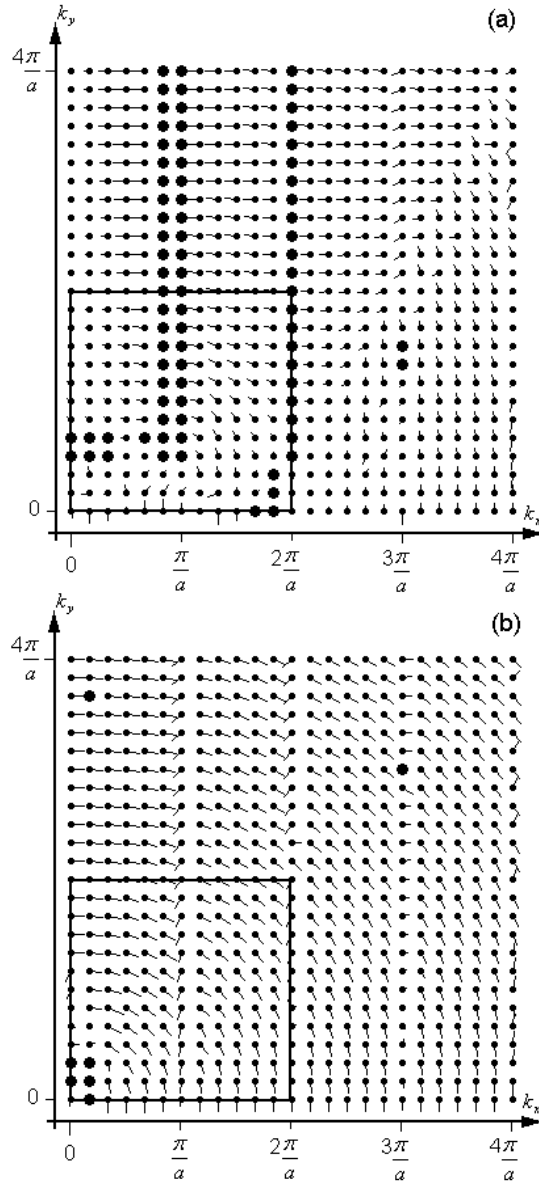


FIG. 3: Distribution of spin mean values for the transmitted state as a function of the point in the (k_x, k_y) plane labeling the incident state for (a) "down" and (b) "up" Rashba bands (3) for the amplitude of the superlattice periodic potential $V_0 = 2$ meV. The incoming states having the energy which falls in the energy gap of the superlattice spectrum are labeled by black circles. These points manifest itself as the points of total reflection since the corresponding incident states are not transmitted through the superlattice. The detailed spin distribution in the insets is shown in Fig.4a and Fig.5a.

incoming state with "down" or "up" polarization. Correspondingly, in Fig.4b and Fig.5b we show the minimal difference between the energy of the incoming state and the band energy of the SO superlattice. Flat areas describe the propagating state when the energy difference is zero and one can find the states in the superlattices having

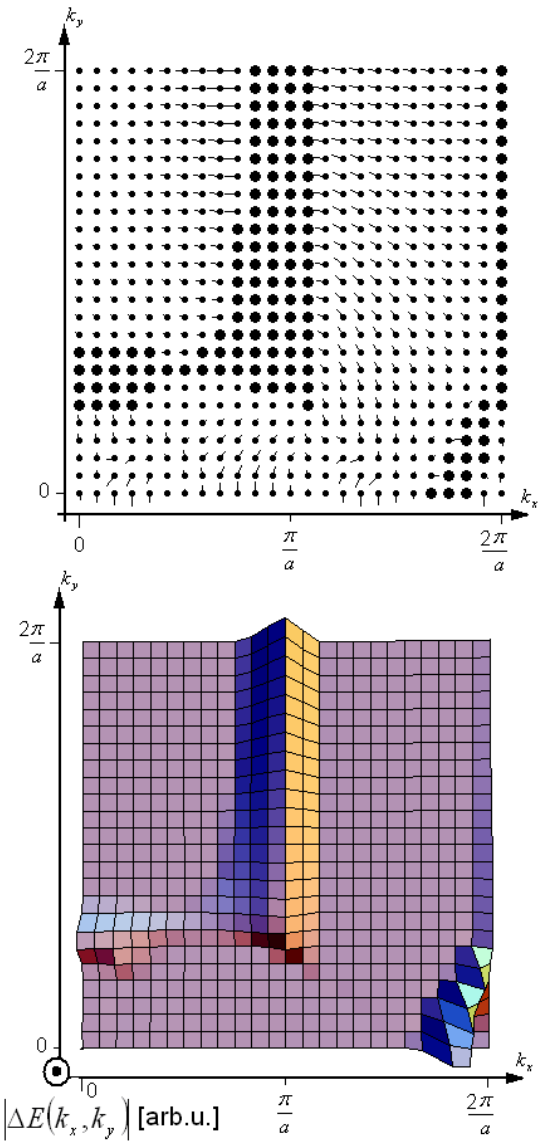


FIG. 4: The inset from Fig.3a showing (a) the spin mean values distribution and (b) minimal difference between the energy of the incoming wave and the band energy of the superlattice. The transmitted waves have the well-defined spin projections in (a) which correspond to the flat parts of the 3D plot in (b) with zero $|\Delta E|$ shown along z axis. The areas of total internal reflection shown as black circles in (a) correspond to the "hills" in (b) with non-zero energy distance between the energy of the incident wave and the nearest superlattice band at fixed k_y .

the same energy as the incident wave. These flat areas correspond to the regular points in Fig.4 and Fig.5 away from the black circles. Then, if the energy of the incoming state falls inside the energy gap of the superlattice, one finds the energy difference in Fig.4b and Fig.5b to be nonzero which is shown along the z axis. By comparing Fig.4a,b and Fig.5a,b one can clearly establish the black circles in Fig.4a and Fig.5a with the "hills" in Fig.4b

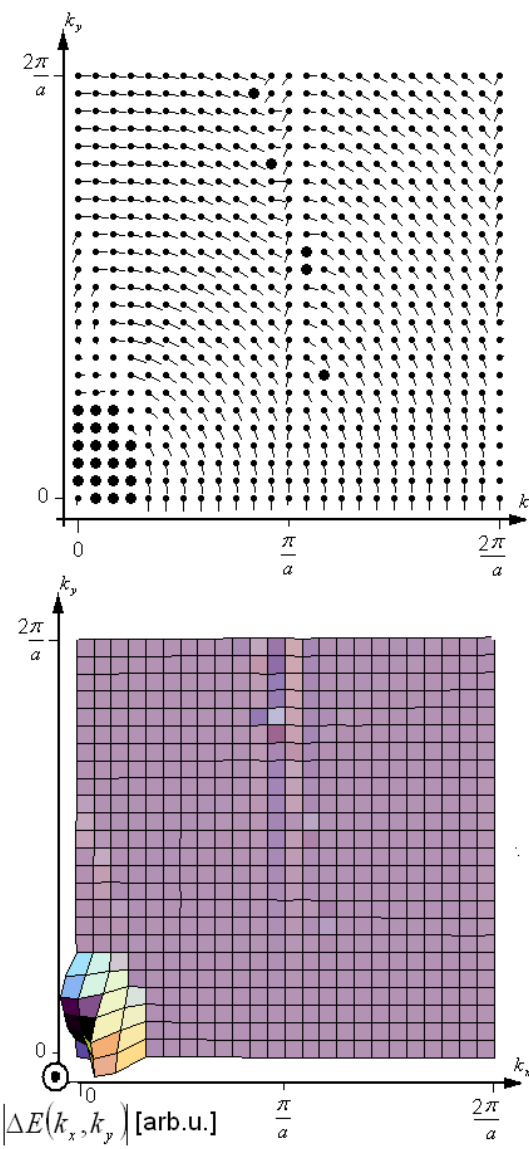


FIG. 5: The same as Fig.4 but for the "up" polarized Rashba incident state.

and Fig.5b. Thus, the areas of total internal reflection correspond to the energy gaps in the SO superlattice. By looking on Fig.3 one can see that some part of these points is clustered near the lines $k_x = \pi n/a$, $n = 1, 2, \dots$ which correspond to the Brillouin zone borders. Since it is well known that at such points the opening of energy gaps is highly probable, the areas of total reflection follow the pattern of Brillouin zones for the superlattice.

When the amplitude of the external gate potential V_0 is increased, the energy gaps also grow up which is followed by the expansion of the areas of total reflection. An example of such expansion is given in Fig.6 where the spin distribution is shown for the same limits in the reciprocal space describing the incident wave but with greater amplitude of the periodic potential $V_0 = 3.5$ meV.

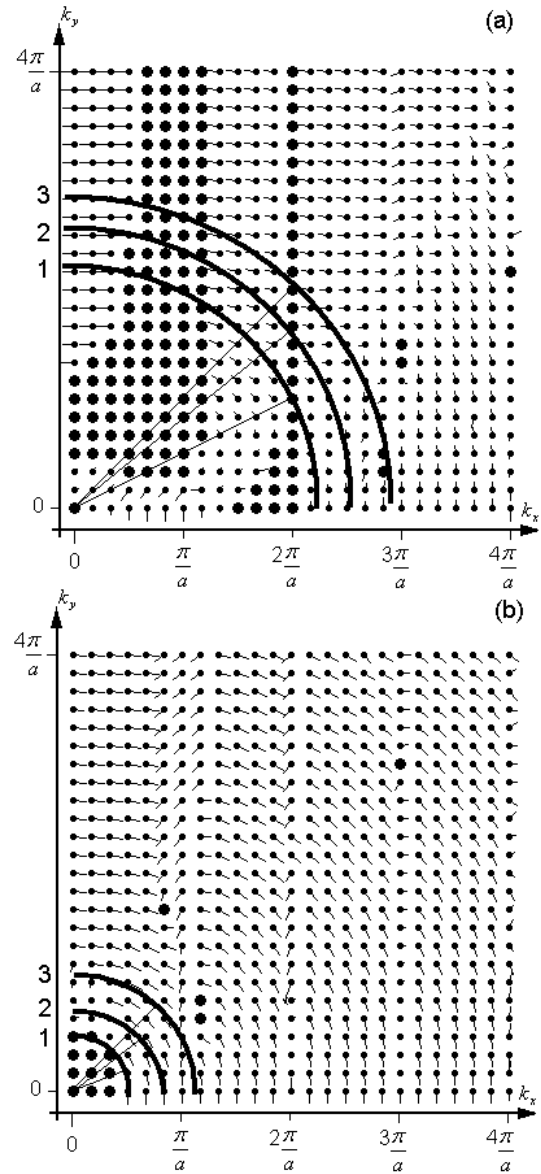


FIG. 6: Spin distribution shown for the same limits in the reciprocal space as in Fig.3 but with $V_0 = 3.5$ meV for (a) "down" and (b) "up" Rashba band. The areas of total reflection occupy the bigger area in the (k_x, k_y) plane which is the result of the expanded energy gaps. Three semi-arch curves correspond to three Fermi energy contours for the incident state where the energy grows from contour 1 to contour 3. In Fig.(a) the marked directions of incidence correspond to the points of total reflection while in Fig.(b) the transmitted state exist at the same Fermi energy, leading to the spin filtering.

One can see that the areas of total reflection occupy the bigger area in the (k_x, k_y) plane which is the result of the expanded energy gaps. Three semi-arch curves correspond to three Fermi energy contours for the incident state where the energy grows from contour 1 to contour 3. The Fermi radii for the down- and up- Rashba bands shown in Fig.6a and Fig.6b, respectively, are shifted by

the constant value $2m\alpha$. Considering three different angles of incidence for each of the Fermi contours in Fig.6 which directions are shown by the straight lines one can see that along these directions the Fermi contours for the down- Rashba band in Fig.6a fall into the areas of total reflections marked by the black circles. At the same time, the corresponding points on the Fermi contours for the up- Rashba band shown in Fig.6b do not fall into the energy gaps of the superlattice and have the defined spin projections for the angles of incidence considered in our example. Thus, the results in Fig.6 demonstrate that the initial flow of SO split electrons at given Fermi energy which consists of down- and up- Rashba contributions with the wavevectors defined in (4) and with opposite spin projections can be filtered at certain angles of incidence by the SO superlattice and converted into the state having only one defined mean spin value. Such feature of the SO superlattice may be used for the further applications of the SO superlattice in the problems of spin detection and control.

VI. CONCLUSIONS

We have studied the scattering of two-component spinors on the spin-orbit lateral superlattice. The in-

coming and reflected states were considered as the two-component eigenstates of Rashba Hamiltonian while the transmitted states in the superlattice were the Bloch spinors. The areas of propagation and total reflection of spin-polarized states were found as a function of incident electron polarization and momentum. For the transmitted states we calculated the mean spin values as a function of the polarization and wavevector of the incoming states and discussed the possible spin filtration mechanism. The results are promising for the applications in controllable spin transmission which can be achieved by the spin-orbit superlattice linked to the two-dimensional electron gas in a semiconductor structure.

Acknowledgments

The author thanks V.Ya. Demikhovskii for numerous fruitful discussions. The work was supported by the Program "Development of the Higher school research potential" RNP.2.2.2.3.928, by the Russian Foundation for Basic Research Grant No.05-02-16449, by the CRDF Award RUX0-001-NN-06, and by the Dynasty Foundation Young Ph.D. Grant (2006).

* Electronic address: khomitsky@phys.unn.ru

¹ E.I. Rashba, Fiz. Tverd. Tela (Leningrad) **2**, 1224 (1960) [Sov. Phys. Solid State **2**, 1109 (1960)]; Y.A. Bychkov and E.I. Rashba, J. Phys. C **17**, 6039 (1984).

² I. Zutić, J. Fabian, and S. Das Sarma, Rev. Mod. Phys. **76**, 323 (2004).

³ S. Datta and B. Das, Appl. Phys. Lett. **56**, 665 (1990).

⁴ A.V. Moroz and C.H.W. Barnes, Phys. Rev. B **60**, 14272 (1999).

⁵ F. Mireles and G. Kirczenow, Phys. Rev. B **64**, 024426 (2001).

⁶ M. Governale and U. Zülicke, Phys. Rev. B **66**, 073311 (2002).

⁷ X.F. Wang and P. Vasilopoulos, Phys. Rev. B **67**, 085313 (2003).

⁸ X.F. Wang, Phys. Rev. B **69**, 035302 (2004).

⁹ S. Debal and B. Kramer, Phys. Rev. B **71**, 115322 (2005).

¹⁰ P.Kleinert, V.V.Bryksin, O. Bleibaum, Phys. Rev. B **72**, 195311 (2005).

¹¹ J.B. Miller, D.M. Zumbühl, C.M. Marcus, Y.B. Lyanda-Geller, D. Goldhaber-Gordon, K. Campman, and A.C. Gossard, Phys. Rev. Lett. **90**, 076807 (2003).

¹² M. Khodas, A. Shekhter, and A.M. Finkel'stein, Phys. Rev. Lett. **92**, 086602 (2004).

¹³ A. Shekhter, M. Khodas, and A.M. Finkel'stein, Phys. Rev. B **71**, 125114 (2005).

¹⁴ V.Ya. Demikhovskii and D.V. Khomitsky, JETP Letters **83**, iss.8, p.340 (2006) [Pis'ma v ZhETF **83**, iss.8, p.399 (2006)].

¹⁵ E.T. Goodwin, Proc. Cambridge Philos. Soc. **35**, 221 (1939).

¹⁶ S.D. Kevan, N.G. Stoffel, and N.V. Smith, Phys. Rev. B **32**, 4956 (1985).

¹⁷ H. Ohno, E.E. Mendez, J.A. Brum, J.M. Hong, F. Agulló-Rueda, L.L. Chang, and L. Esaki, Phys. Rev. Lett. **64**, 2555 (1990).

¹⁸ H.K. Sy and T.C. Chua, Phys. Rev. B **48**, 7930 (1993).

¹⁹ J. Kłos and H. PuszkarSKI, Phys. Rev. B **68**, 045316 (2003).